Available online at www.sciencedirect.com
ScienceDirect
Developmental Biology 311 (2007) 434–448
DEVELOPMENTAL BIOLOGY
www.elsevier.com/developmentalbiology

Apoptosis regulates notochord development in *Xenopus*

Marina A. Malikova [a], Melanie Van Stry [b], Karen Symes [a,*]

[a] *Department of Biochemistry, Boston University School of Medicine, Boston, MA, USA*
[b] *Department of Immunology, St. Jude Children's Research Hospital, Memphis, TN, USA*

Received for publication 11 July 2007; revised 22 August 2007; accepted 27 August 2007
Available online 5 September 2007

Abstract

The notochord is the defining characteristic of the chordate embryo and plays critical roles as a signaling center and as the primitive skeleton. In this study we show that early notochord development in *Xenopus* embryos is regulated by apoptosis. We find apoptotic cells in the notochord beginning at the neural groove stage and increasing in number as the embryo develops. These dying cells are distributed in an anterior to posterior pattern that is correlated with notochord extension through vacuolization. In axial mesoderm explants, inhibition of this apoptosis causes the length of the notochord to approximately double compared to controls. In embryos, however, inhibition of apoptosis decreases the length of the notochord and it is severely kinked. This kinking also spreads from the anterior with developmental stage such that, by the tadpole stage, the notochord lacks any recognizable structure, although notochord markers are expressed in a normal temporal pattern. Extension of the somites and neural plate mirrors that of the notochord in these embryos, and the somites are severely disorganized. These data indicate that apoptosis is required for normal notochord development during the formation of the anterior–posterior axis, and its role in this process is discussed.

Keywords: *Xenopus*; Embryo; Apoptosis; Notochord; Embryonic axis; Bcl-2

Introduction

The notochord is the defining characteristic of the chordate embryo. It develops at the midline during gastrulation and persists as a long, flexible rod that underlies the neural tube and extends through most of the length of the embryo. The notochord plays crucial roles throughout embryonic development, acting as a signaling center that provides position and fate information for all three embryonic germ layers (Christ et al., 2004; Cleaver and Krieg, 2000; Cunliffe and Ingham, 1999; Danos and Yost, 1995; Fouquet et al., 1997; Goldstein and Fishman, 1998; Lohr et al., 1997; Münsterberg and Lassar, 1995; Pourquie et al., 1993; Stemple, 2005; Yamada et al., 1991, 1993), and structurally as a primitive skeleton (Adams et al., 1990; Bruns and Gross, 1970). In most vertebrates the notochord is a transient structure, the remnants of which form the nucleus pulposus of the intervertebral discs of the spine (Christ et al., 2000; Pourquie et al., 1993; Rufai et al., 1995; Smits and Lefebvre, 2003; Theiler, 1988).

In *Xenopus*, the notochord is formed through cell intercalation (convergent extension) of the prospective axial mesoderm (Keller et al., 2003). It is distinguished early by the characteristic shape and packing of its cells, which resembles a stack of pizzas with each cell constituting a slice with the pointed end of each cell directed toward the inside of a round notochord (stage 20) (Keller et al., 1989; Keller, 1984; Youn and Malacinski, 1981). From this stage, convergent extension is thought to be less important for notochord lengthening (Keller et al., 1989) and no cell division takes place (Keller et al., 1989). During development, the notochord becomes encased in a fibrous sheath and its cells become vacuolated and enlarged. The vacuoles contain secreted glycosaminoglycans (Waddington and Perry, 1962) that have been proposed to increase vacuole size by promoting the osmotic uptake of water (Adams et al., 1990). In *Xenopus*, this vacuolization begins during the tailbud stages (stages 23–24) (Nieuwkoop and Faber, 1967) proceeding in an anterior to posterior direction and contributing to the length of the notochord (Adams et al., 1990; Keller et al., 1989). Vacuolization is not complete until the embryo becomes a tadpole (stage 37/38) (Nieuwkoop and Faber, 1967).

* Corresponding author.
E-mail address: symes@bu.edu (K. Symes).

0012-1606/$ - see front matter © 2007 Elsevier Inc. All rights reserved.
doi:10.1016/j.ydbio.2007.08.047

The notochord's role as a signaling center is a well-recognized component of normal embryonic development (Stemple, 2005), however, its structural role is equally important. For example, the lengthening of axial tissues such as the neural plate depends on notochord extension. Extirpation of the notochord reduces the elongation of the embryo in the regions where it is removed in amphibians (Horstadius, 1944; Kitchen, 1938, 1949; Nieuwkoop, 1947), chicks (Jacobson, 1981) and ascidians (Reverberi et al., 1960). In addition, convergent extension of the neural plate is weak unless it is explanted with notochord in *Xenopus* (Elul and Keller, 2000; Ezin et al., 2003). Zebrafish embryos with mutations in genes that are necessary for the differentiation of chordamesoderm into mature notochord, such as bashful (*bal*), grumpy (*gup*) and sleepy (*sly*), have a shortened anteroposterior axis (Odenthal et al., 1996; Stemple et al., 1996). Similarly, mutations in sneezy (*sny*), happy (*hap*) and dopey (*dop*) that encode the α, β or γ chains of the laminin coatomer complex, respectively, cause a loss of notochord basement membrane and a failure of vacuole formation that also results in embryos with a shortened anteroposterior axis (Coutinho et al., 2004). Curly tail (*ct*) mutant mice develop with tail curvature and a high frequency of open neural tubes. This is due to a mismatch in the growth rates of neural tubes and notochord–endoderm tissues (Copp et al., 1988a,b). These defects are corrected by reducing the growth rate of both components to a uniformly low value (Copp et al., 1988b), suggesting that the difference in extension rates in the two tissues is the primary cause of the failure of the neural tube to close.

The presence of apoptotic cells in the notochord of tadpole stage *Xenopus* embryos (stages 29–35) (Hensey and Gautier, 1998), zebrafish embryos beginning at 14 h post fertilization (Cole and Ross, 2001) and chick embryos H.H. stage 9 (Hirata and Hall, 2000) has been reported. In *Xenopus*, this cell death is prevented by the overexpression of the anti-apoptotic factor Bcl-2 suggesting that it occurs through the mitochondrial apoptotic pathway (Yeo and Gautier, 2003). Recent evidence suggests that the death-receptor apoptotic pathway may also play a role in the development of tailbud embryos (Morgan et al., 2004). It has been shown that Hoxb4 directly induces the expression of FLASH in the notochord after neurulation. FLASH is a component of the FAS–caspase-8 apoptotic pathway, and blocking Hoxb4 or FLASH prevents apoptosis in the notochord of stage 28 embryos (Morgan et al., 2004). In addition, caspases-1–3 and caspases-6–10 have been cloned in *Xenopus* (Nakajima et al., 2000) suggesting that both death receptor and mitochondrial–apoptosis pathways likely operate during their development. Apoptotic cells are usually removed from developing tissues by phagocytosis by macrophages and by neighboring cells expressing the phosphatidylserine receptor (Hong et al., 2004). Prevention of the removal of cell corpses by inhibition of the phosphatidylserine receptor results in a variety of developmental defects, including malformation of the notochord (Hong et al., 2004). This suggests that apoptosis in the notochord and subsequent removal of those cells is necessary for normal morphogenesis of this tissue.

Apoptosis is a well-documented part of normal development in a number of tissues. For example, during the development of the vertebrate central and peripheral nervous systems, a large percent of differentiated neurons die (Patterson, 1992; Raff et al., 1993). Apoptosis is also utilized in several regions to sculpt the tetrapod limb including the separation of the digits and the formation of the radius and ulna (Mori et al., 1995; Saunders and Fallon, 1966; Zuzarte-Luis and Hurle, 2005). In addition, embryonic cavities can be formed by apoptosis such as by death of the epiblast cells in the developing mouse embryo (Coucouvanis and Martin, 1995). In mammalian embryos, cells from the notochord are lost as it is remodeled to form the nucleus pulposus of the intervertebral discs (Glucksmann, 1951). It has been proposed that this process involves apoptosis (Cotten et al., 1994; Glucksmann, 1951; Goto and Uhthoff, 1986; Kim et al., 2005), but the evidence for this is controversial (Aszodi et al., 1998). The work presented here, however, is the first to show that cell death is a normal and critical component of early notochord development.

We found that there is little or no cell death in the mesoderm prior to the neural groove stage. Beginning in the late neurula and continuing throughout the tailbud stages, apoptosis increases in the notochord with an anterior to posterior progression. Prevention of this apoptosis by the overexpression of Bcl-2 mRNA causes an increase in the length-to-width ratio and the notochord length is approximately doubled in dorsoanterior mesoderm explants. In intact embryos, inhibition of apoptosis results in a deformed notochord. The length of the notochord in these embryos is not increased, however, the notochord is severely kinked. This kinking also appears in an anterior to posterior pattern with developmental stage. These disruptions in structure are not the result of developmental delay because notochord markers are expressed in a normal temporal pattern. However, the development of surrounding tissues is affected, with the extension of the somites and neural plate mirroring that of the notochord and the somites failing to organize correctly. These data indicate that apoptosis is an important regulator of notochord development during axis elongation and its role in this process is discussed.

Materials and methods

Embryos

Xenopus embryos were fertilized in vitro, dejellied in 2% cysteine, pH 7.8, and cultured in 10% Marc's Modified Ringer (0.1× MMR) (Peng, 1991) at temperatures between 14 °C and 23 °C as previously described (Ataliotis et al., 1995). Embryos were staged according to Nieuwkoop and Faber (1967).

mRNA synthesis and microinjection

mRNA for microinjection was transcribed from template DNA with the mMessage mMachine kit (Ambion). Microinjections were carried out in a solution of 3% Ficoll in 1× MMR (Peng, 1991). At the 4-cell stage, embryos were injected into the marginal zone of each dorsoanterior blastomere with 1 ng or 0.5 ng Bcl-2 mRNA for explants and whole embryo experiments, respectively, and 0.5 ng GAP43-GFP mRNA (encoding green fluorescent protein with a membrane localization signal) as a lineage tracer (the kind gift of Eddie De Robertis) (Kim et al., 1998; Moriyoshi et al., 1996).

Microdissection

Open-faced Keller explants were dissected, cultured and analyzed as described previously (Tahinci and Symes, 2003). Briefly, explants were dissected at stage 10.25 from embryos that had been microinjected at the 4-cell stage (see above). Only embryos with GFP localized to the dorsoanterior marginal zone were used for dissection of explants. Explants were held flat under a coverslip bridge and cultured in 1× Danilchik's for Amy (DFA) at 14 °C until sibling stage 25 (Sater et al., 1993). The explants were then photographed (Zeiss Stemi SV6-GFP). Explant extension was assessed double blind and by calculating the ratio of the longest aspect of each explant to its width at the constriction point where the mesoderm extends from neural ectoderm (LWR; Fig. 3A) (Wallingford et al., 2001). In addition, the length of the notochord was measured. All measurements were performed using the public domain NIH image 1.62 program (http://rsb.info.nih.gov/nih-image/). The LWR and notochord length in these explants were statistically analyzed using the unpaired Student's t test (Dawson and Trapp, 2004) at the level of significance $\alpha=0.05$. The mean and standard error were calculated and differences found between treated and control values were considered statistically significant if $p<0.05$. The biostatistics program SPSS version 14.0 (SPSS Inc.) was used to perform the test. The explants were then fixed in MEMFA for 1–2 h at 4 °C, rinsed in PBS and stored in methanol at −20 °C prior to immunohistochemistry and TUNEL staining.

Wholemount immunohistochemistry

The monoclonal antibody Tor70 (the kind gift of Richard Harland) (Bolce et al., 1992; Kushner, 1984) was used to identify the notochord in open-faced Keller explants and whole embryos at different stages of embryonic development.

Briefly, explants or embryos were rehydrated through a methanol/PBS series. Nonspecific immunoglobulin-binding sites were then blocked by incubation at room temperature in PBT (PBS with 0.5% BSA and 0.1% Triton X-100) with 10% goat serum for 1 h. The explants or embryos were incubated in 1:10 dilution of Tor70 at 4 °C overnight. After several washes, they were blocked in PBT with 10% goat serum and incubated in the secondary antibody Cy3-conjugated goat anti-mouse IgM (1:500 dilution; Jackson Immunoresearch) overnight at 4 °C and then washed in PBT before being stored in methanol at −20 °C. To visualize GFP, somitic mesoderm, neural tube or laminin the embryos were further processed for immunohistochemistry with an Alexa-488 conjugated anti-GFP antibody (Molecular Probes, Invitrogen; 1:100 dilution), or 12/101 (Developmental Studies Hybridoma Bank; 1:20 dilution) (Kintner and Brockers, 1984) or Xen1 (3B1) (Developmental Studies Hybridoma Bank; 1:5 dilution) (Ruiz i Altaba, 1992) followed by FITC goat anti-mouse IgG (1:500 dilution; Jackson Immunoresearch) or anti-laminin (Sigma; 1:25 dilution) followed by Alexa Fluor 488 goat anti-mouse IgG (Invitrogen; 1: 500 dilution), respectively. Embryos and explants were then either processed for TUNEL staining, cleared using a 2:1 ratio of benzyl benzoate to benzyl alcohol (BB:BA) for measurement of notochord length using NIH image (see below), or fixed in MEMFA for 2 h at 4 °C and processed for histology in JB4 according to manufacturer's instructions (Polysciences).

Wholemount in situ hybridization

Embryos at stage 23 or 35/37 that had been injected with Bcl-2 and/or GFP mRNA as described above were processed for wholemount in situ hybridization as described by Harland (1991). Digoxigenin-labeled cRNA probes for the early notochord marker axial protocadherin (AXPC) (Kim et al., 1998) or the late notochord marker procollagen IIA (Su et al., 1991) were used to examine notochord development. Embryos were then post fixed in MEMFA and processed for histology as described above.

TUNEL staining

Wholemount TUNEL staining of embryos was carried out following fixation for 1 h in MEMFA at 4 °C or after immunohistochemistry using the In Situ Cell Death Detection Kit, POD (Roche Molecular Biochemicals) as previously described (Van Stry et al., 2004). Briefly, embryos were treated for 1 h in 3% hydrogen peroxide in methanol to inhibit endogenous peroxidase activity, rinsed in PBS and permeabilized in 0.1% Triton-X 100 in 0.1% sodium citrate for 30 min on ice. The embryos were rinsed in PBS and placed in the TUNEL reaction mixture at 37 °C overnight for nicked-end labeling. As a positive control, permeabilized embryos were incubated with 2 units of DNase I (Promega) for 30 min at 37 °C prior to the labeling reaction. The embryos were rinsed in PBS, blocked with 20% goat serum in PBT, and incubated overnight at 4 °C with the Converter–POD solution (anti-fluorescein HRP conjugated antibody). Prior to staining, the embryos were rinsed overnight in PBS. For the chromogenic horseradish peroxidase reaction, the embryos were transferred to DAB substrate in DAB buffer as described by the manufacturer (Roche Molecular Biochemicals) for 30 min to 1 h. The reaction was stopped by the addition of PBS. The embryos were then stored in methanol at −20 °C before being embedded in JB4 (Polysciences) according to manufacturer's instructions and sectioned (JB4 Sorvall).

Wholemount TUNEL staining of Keller explants was performed as described above for embryos, except for the following changes. Prior to TUNEL staining the explants were rehydrated through a methanol/PBS series. In addition, TUNEL-positive, fluorescein-labeled cells were viewed directly using an SV6-GFP Microscope (Zeiss).

Measurements

Notochord disruptions along the anteroposterior axis were assessed in wholemount (see Supplemental Table 1) and in histological sections (see Supplemental Table 2) within 4 sectors that encompassed the percent of the notochord from the anterior, 0–25%, 26–50%, 51–75% and 76–100%. In addition, the following were used to score the severity of the phenotype in histological section (see Supplemental Table 2): − for normal, + for a mild phenotype including a rippled notochord with contiguous borders, ++ for highly kinked notochord but with contiguous borders and +++ for severe phenotypes including breakages in the notochord borders and a loss of internal structure. To present these data quantitatively, the following numbers were assigned to each category of disruption, grade 0 for −, grade 1 for +, grade 2 for ++ and grade 3 for +++. The probability of occurrence of each level of notochord disruption (grades 0–3) along anteroposterior axis was assessed using Fisher's exact test (Dawson and Trapp, 2004). The data were compared in 2×2 cross tables, which were set up individually for each notochord segment (0–25%, 26–50%, 51–75%, 76–100%) in Bcl-2-injected embryos for each developmental stage examined (stages 19, 23, 30 and 35). The corresponding segment in a stage control GFP-injected embryo was used as the reference group. The test was performed at the level of significance $\alpha=0.05$. Observations were considered to be statistically significant if $p<0.05$. The biostatistics program SPSS version 14.0 (SPSS Inc.) was used to perform the tests.

Results

Apoptosis of notochord cells occurs in a temporal anterior to posterior pattern during the tailbud stages of development

To identify the normal pattern of apoptosis in the mesoderm, embryos were fixed, TUNEL-stained and sectioned at different stages of development (stages 15–25). We found TUNEL-positive cells in the notochord but not the somites (Figs. 1A, B). This cell death begins at stage 18 (Fig. 1C), and the number of dying cells increases until at least stage 25 (Fig. 1C). In addition, the spatiotemporal distribution of these apoptotic cells is correlated with notochord development, with the cell death beginning anteriorly and spreading posteriorly with embryonic stage (Figs. 2A, B). For example, at stage 19 apoptotic cells are present largely in the anterior-most notochord, but by stage 25 the majority of dying cells are observed in the posterior

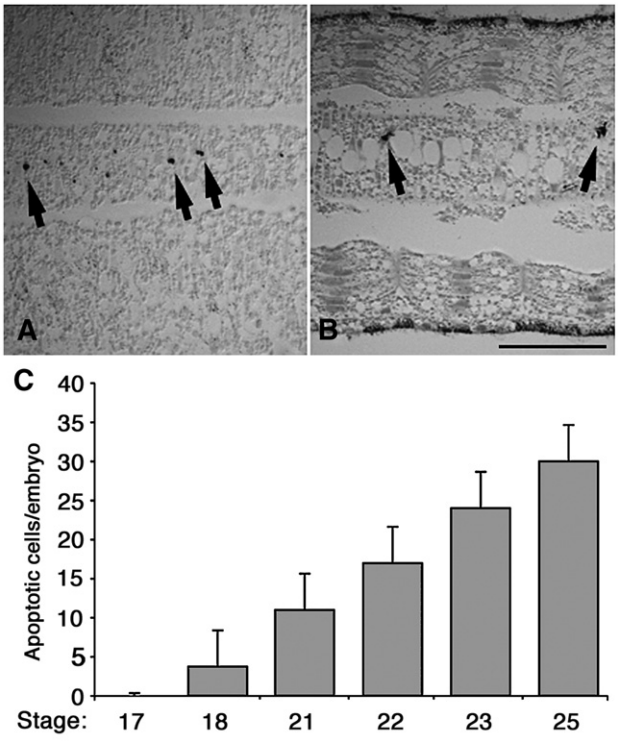

Fig. 1. Apoptosis occurs in the notochord but not somitic mesoderm. Cell death was assessed in intact embryos at different stages of development by TUNEL assay, in which nicked DNA is visualized by terminal-UTP-nicked-end labeling. Longitudinal sections indicating anterior notochord (center) and somites (top and bottom of frames) at stages 21 (A) and 25 (B) are shown. Note the presence of apoptotic cells in the notochord (arrows) but not in the somites. Anterior is to the right in both frames. (C) Graph indicating the number of apoptotic cells in the notochord at stages 17–25. Error bars indicate 95% confidence intervals. A minimum of 8 embryos in 3 independent experiments were used for this analysis. Scale bar in panel B is 100 μm.

notochord, although there are apoptotic cells along the notochord's length (Fig. 2A). Interestingly, this pattern of cell death slightly precedes but overlaps with the vacuolization of notochord cells (Fig. 2B), the major force of notochord extension during these stages of development, suggesting a potential mechanism to limit the extent of this process during normal development.

Apoptosis regulates notochord extension in open-faced Keller explants

To identify the role of apoptosis in the notochord, cell death was blocked in mesoderm explants. Embryos were injected into the prospective dorsoanterior mesoderm with mRNA encoding the anti-apoptotic factor Bcl-2 at the 4-cell stage, which inhibits apoptosis until at least stage 35 (see Fig. 6). Open-faced Keller explants were then dissected at stage 10.25 and cultured until stage 25 when the length-to-width ratio (LWR) was calculated (Fig. 3A). Explants in which apoptosis had been prevented have an LWR almost double that of control explants (Figs. 3B, E). In addition, the length of the notochord is also doubled when cell death is inhibited in these explants (Figs. 3C–F). These data suggest that the elimination of notochord cells through apoptosis regulates the development of this tissue.

Apoptosis regulates the structure of the developing notochord in vivo

To identify the role of apoptosis in vivo, embryos were injected into the presumptive notochord region at the 4-cell stage with mRNA encoding Bcl-2 or GAP43-GFP, as a control. Previous studies have shown that the overexpression of Bcl-2 in *Xenopus* can cause the embryos to develop with spina bifida (Van Stry et al., 2004). To avoid this phenotype, the embryos were monitored throughout their early development to ensure that gastrulation and neurulation occurred normally, however, the Bcl-2-injected embryos developed with severely arched backs (Figs. 4D–F), compared to control embryos (Figs. 4A–C). The embryos were then fixed at different stages (18–35), subjected to wholemount immunohistochemistry using the notochord antibody, Tor70 (for example see Figs. 4C, F), and an anti-GFP antibody (for example see Figs. 4B, E), and the length of the notochord was assessed.

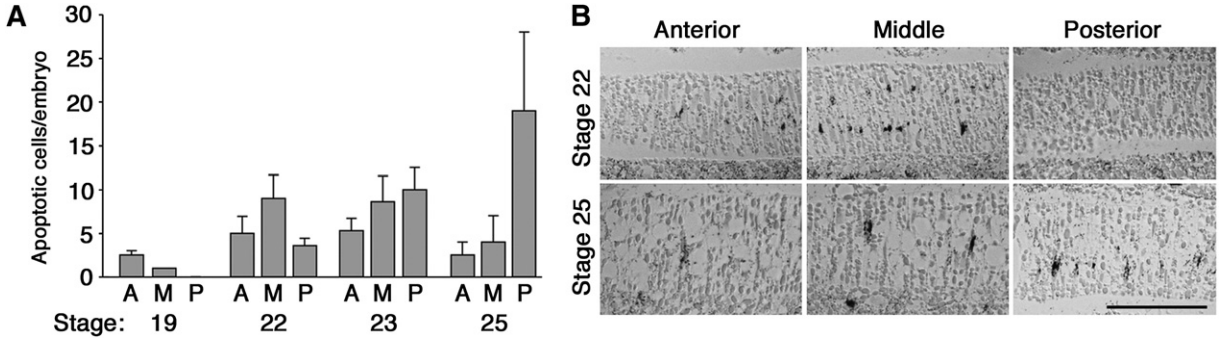

Fig. 2. Apoptosis in the notochord proceeds in an anterior to posterior direction. Embryos were fixed at stages 19–25, TUNEL stained, embedded and sectioned sagittally. (A) The anteroposterior distribution of TUNEL-positive cells in the notochord was assessed in each sagittal section at different developmental stages and notochord positions (A = anterior; M = middle; P = posterior). Error bars indicate 95% confidence intervals. (B) TUNEL-stained, sagittal sections of notochord at stages 22 (top panels) and 25 (bottom panels). Anterior, middle and posterior regions of the notochord are shown. At stage 25 the anterior and middle regions are fully vacuolated. Note the A to P change in the distribution of apoptotic nuclei with developmental stage. A minimum of 8 embryos in 3 independent experiments were used for this analysis. Scale bar in panel B is 100 μm.

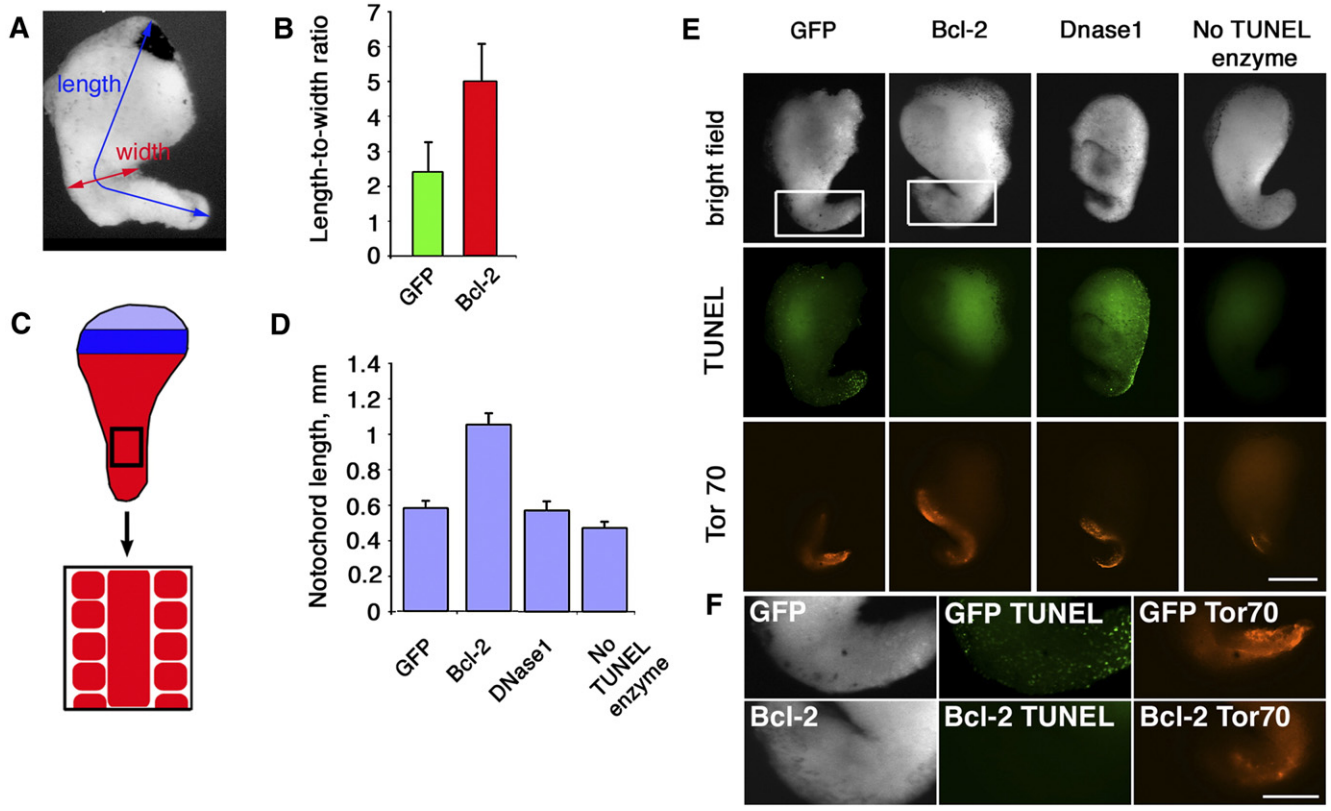

Fig. 3. Apoptosis regulates the extension of axial mesoderm explants. Embryos were injected with either Bcl-2 or GFP mRNA into the dorsoanterior marginal zone at the 4-cell stage. Open-faced Keller explants were dissected at stage 10.25 and cultured until sibling embryos reached stage 25, when they were fixed and analyzed. (A) The length-to-width ratio (LWR) of axial mesoderm explants was assessed by calculating the ratio of the longest aspect of each explant (length) to its width at the constriction point where the mesoderm extends from neural ectoderm. (B) The LWR of axial mesoderm explants derived from embryos microinjected with control (GFP, $n=31$) or Bcl-2 ($n=34$) mRNA was calculated. Note that explants in which apoptosis was prevented by Bcl-2 injection have a greater LWR than control explants. (C) Open-faced Keller explants comprise the prospective ectoderm ( ), neural ectoderm ( ) and mesoderm ( ). Following convergent extension, differentiated notochord is flanked by somites (represented enlarged in the indicated box). (D) The length of the notochord was also measured in control (GFP mRNA-injected ($n=14$), DNase I treated – a positive control for TUNEL assay – ($n=10$) and no TUNEL enzyme – a negative control for TUNEL assay – ($n=8$)) and Bcl-2 mRNA-injected ($n=22$) explants. Note that the notochord in Bcl-2-injected explants elongated to a greater extent than in control explants. (E) Cell death was assessed by TUNEL assay (middle panels). The notochord is visualized by immunohistochemistry using the notochord antibody Tor70 (lower panels). DNase I treated explants are shown as a positive control for the TUNEL assay. Background autofluorescence is visible in all explants. (F) Higher magnification images of area within white boxes in GFP control and Bcl-2 explants shown in panel E. Note that apoptosis of mesoderm cells in mock-injected control explants (TUNEL-positive fluorescein-labeled cells) is blocked in Bcl-2-injected explants. Error bars in panels B and D indicate 95% confidence intervals. Scale bars in panels E and F 500 μm and 200 μm, respectively.

In contrast to open-faced Keller explants, there is a small but significant reduction in notochord length in the Bcl-2-injected embryos compared to controls (Fig. 5A). In addition, notochord morphology is disrupted by severe kinking in the Bcl-2-injected embryos (Figs. 5C, E, G). No kinking is ever seen in control embryos (Figs. 5B, D, F). This kinking

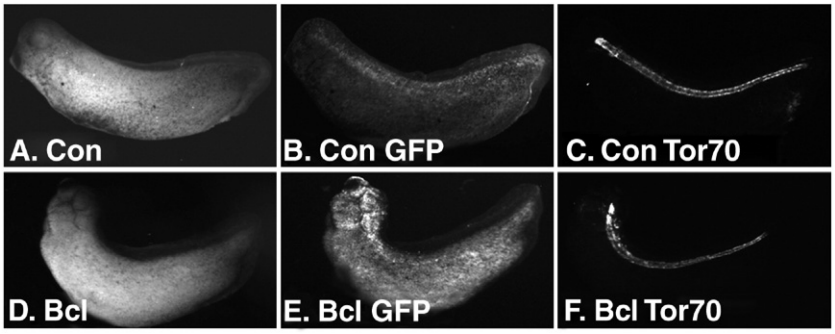

Fig. 4. Inhibition of apoptosis in vivo causes severe arching of the dorsal axis. Embryos were injected into the prospective notochord region with (A–C) control GFP mRNA alone or with (D–F) Bcl-2 mRNA at the 4-cell stage. At stage 30, the embryos were fixed and processed for immunohistochemistry using (B, E) GFP and (C, F) Tor70 antibodies. Note that the embryos that received Bcl-2 mRNA develop with an arched dorsal axis. A minimum of 14 embryos in 3 independent experiments were used for this analysis.

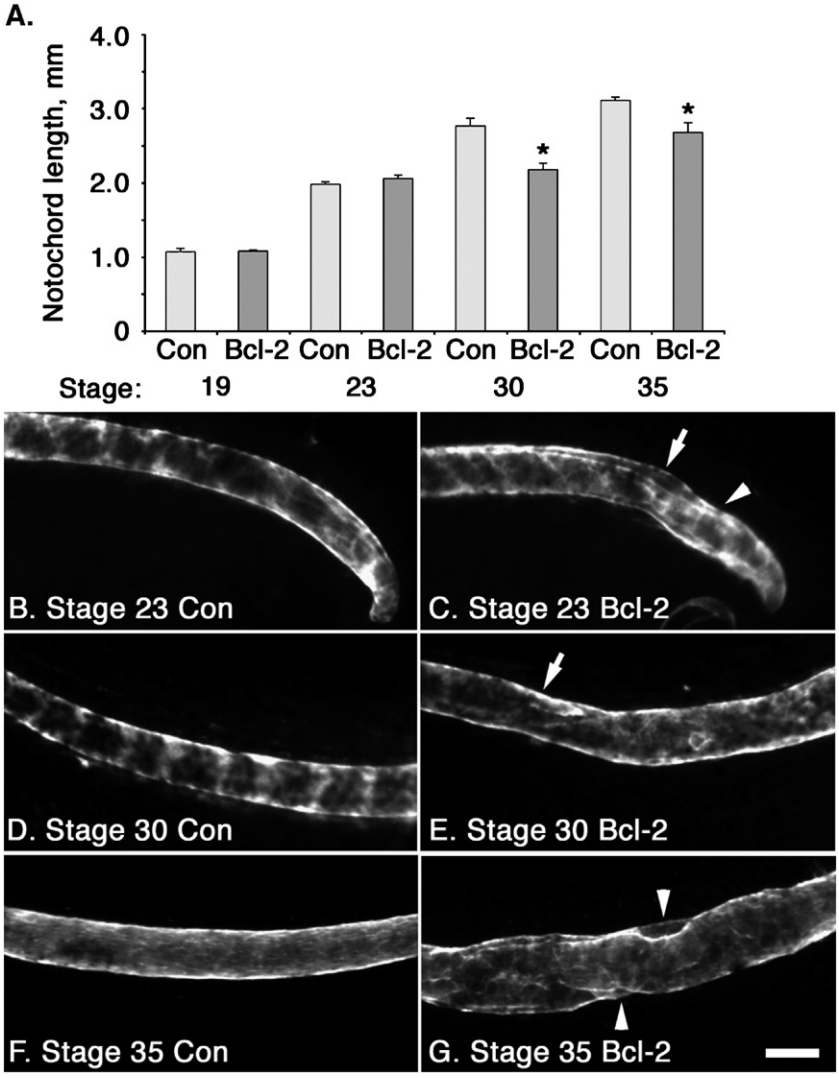

Fig. 5. Inhibition of apoptosis does not increase notochord extension in vivo but causes the notochord to kink severely. Embryos were injected into the prospective notochord region with (A, B, D, F) GFP mRNA (Con) alone or with (A, C, E, G) Bcl-2 mRNA at the 4-cell stage. At stages (A) 19, (A–C) 23, (A, D, E) 30 and (A, F, G) 35 the embryos were fixed and processed for immunohistochemistry using Tor70 and notochord length was measured in wholemount (A). Note that in the embryos that received Bcl-2 mRNA the notochord is kinked (C, E, G; arrowheads in panels C, G) compared to controls (B, D, F). Arrows point to the boundary between kinked and non-kinked notochord (C, E). Error bars indicate 95% confidence intervals. In panel A differences that are statistically significant ($p<0.05$) in the unpaired t test are indicated by *. For stages 23–35 a minimum of 12 embryos in 3 independent experiments were used for this analysis; for stage 19 a minimum of 6 embryos were used. Anterior is to the right. Scale bar in panel G is 100 μm.

begins in the anterior notochord at stage 23 (Fig. 5C, Supplemental Table 1) with the posterior regions similar to the notochord in control embryos. At later stages, however, the notochord is kinked from the anterior, posteriorly. For example, at stage 30, kinks cover the anterior three quarters of notochord (Supplemental Table 1). By stage 35, however, almost the entire notochord is kinked (Supplemental Table 1). At this stage, two kinked phenotypes are observed in approximately equal numbers in the Bcl-2-injected embryos; the notochord is either wider than that in control embryos (compare Figs. 5F and G) or the structure is collapsed (see Fig. 6).

To analyze these phenotypes further, the embryos were TUNEL-stained and then embedded and sectioned (Fig. 6), the extent of vacuolization was determined (Fig. 7), and the anteroposterior position of and severity of the disruptions were assessed at different stages (see Materials and methods; Fig. 8). As described above (Fig. 2A), TUNEL staining revealed that at stage 23 dying cells were present throughout the notochord (Fig. 6A). This cell death was prevented by the overexpression of Bcl-2 (Fig. 6C), the localization of which was inferred from the expression of co-injected GFP mRNA (not shown).

Confirming the data observed in wholemount, analysis of histological sections revealed that inhibition of apoptosis caused extensive disruptions in notochord morphology beginning in the anterior at stage 23 (Figs. 6C, D) and spreading posteriorly with developmental stage (Figs. 6G, H, K, L). In control embryos, the notochord has smooth and continuous edges (Figs. 6A, B, E, F, I, J). In embryos that received Bcl-2 mRNA, however, the notochord is extremely misshapen (Figs.

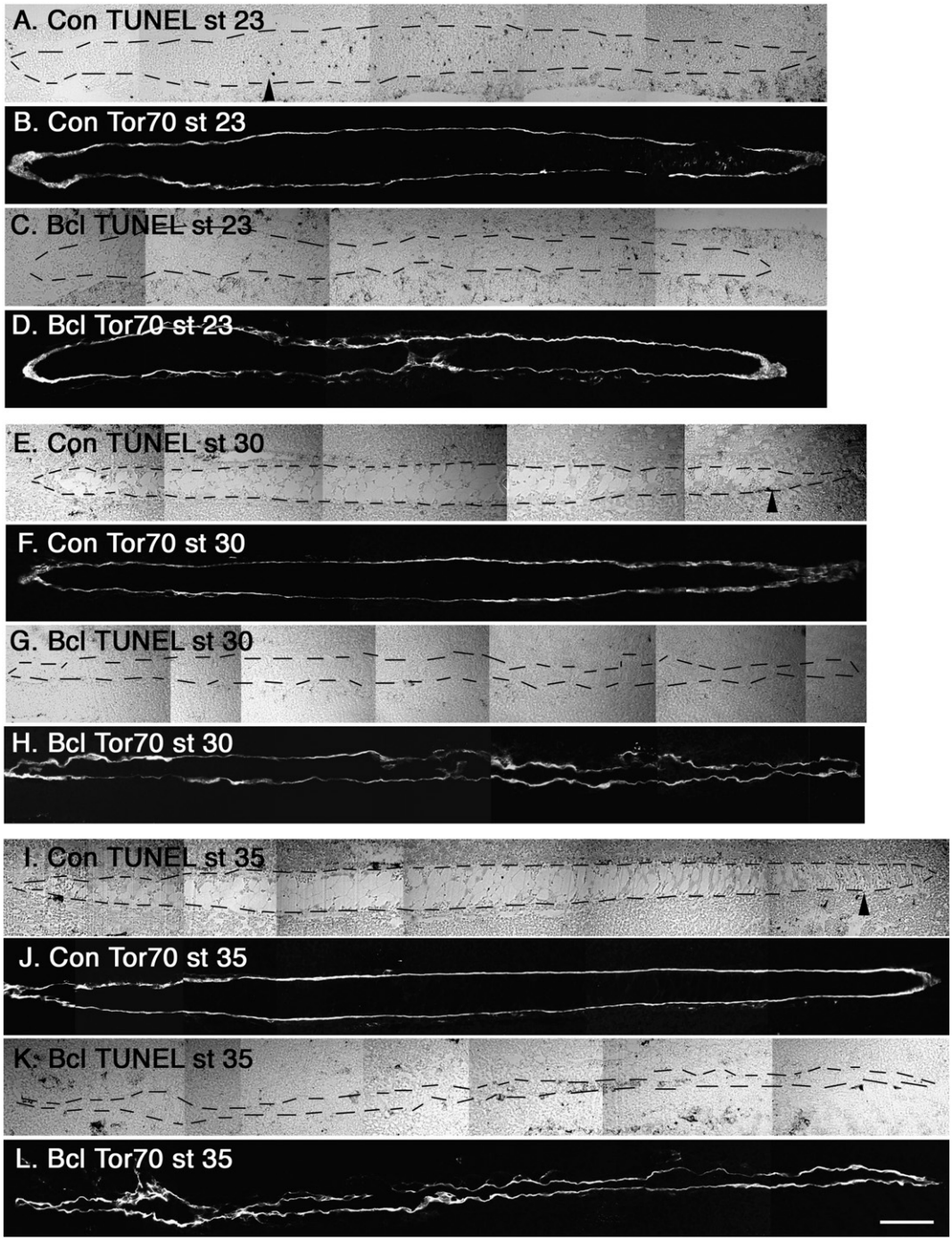

Fig. 6. Inhibition of apoptosis severely disrupts notochord structure. Embryos were injected into the prospective notochord region with (A, B, E, F, I, J) GFP mRNA or (C, D, G, H, K, L) Bcl-2 mRNA at the 4-cell stage. At stages 23 (A–D), 30 (E–H) and 35 (I–L) the embryos were fixed, processed for immunohistochemistry using Tor70, TUNEL stained and then embedded and sagittally sectioned. Note that inhibition of apoptosis by Bcl-2 disrupts the structure of the notochord such that by stage 30, the notochord structure is severely compromised, with extensive kinking and a lack of vacuolization. Arrows in panels A, E and I indicate the anteroposterior limit of vacuolization. Dotted lines indicate the position of the notochord in panels A, C, E, G, I and K. Anterior is to the left in all frames. Scale bar in panel L is 100 μm.

6C, D, G, H, K, L). Like control embryos, at stage 23 the Bcl-2-injected embryos have anterior vacuoles (compare Figs. 6A and C). At stage 30, however, a lack of cell death in the notochord causes it to develop with broken edges and with little to no vacuolization (Figs. 6G, H) and by stage 35, the notochord has lost integrity and, in places, completely collapsed (Figs. 6K, L).

To determine whether these disruptions could be correlated with vacuolization, the anteroposterior limit of vacuoles present in control embryos was identified (Figs. 6A, E, I and 7). At stage 23, the anterior 29% of the notochord is vacuolated (Figs. 6A and 7), and this increases to 91% and 94% by stages 30 and 35, respectively (Figs. 6E, I and 7). Bcl-2-injected embryos were not used for this analysis because it is difficult to

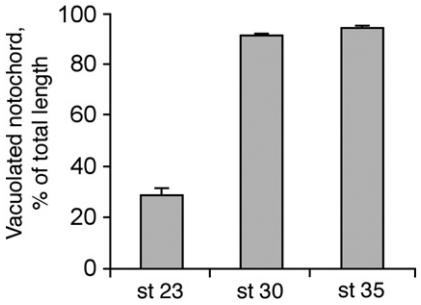

Fig. 7. Anteroposterior limit of notochord vacuolization changes with embryonic stage. Sagittal histological sections of GFP-injected embryos at stage 23, 30 and 35 were examined for the presence of vacuoles in the notochord, which begins in the anterior at stage 23. The anterior–posterior limit of the vacuoles is indicated as a percentage of total notochord length. A minimum of 5 embryos were analyzed at each stage. Error bars indicated 95% confidence interval.

distinguish vacuoles in later staged embryos (see Fig. 9). These data indicate that the kinking of the notochord in Bcl-2-injected embryos and normal vacuolization are coincident, beginning at the same developmental stage and with a similar anterior to posterior progression.

The severity of notochord disruptions in Bcl-2-injected embryos is also increased at later stages (Figs. 6C, D, G, H, K, L, Fig. 8, and Supplemental Table 2). Notochord disruptions along the anteroposterior axis were classified into 4 categories (grades 0–3) according to the severity of the phenotype (see Materials and methods; Fig. 8). The probability of occurrence of each category of disruption in Bcl-2-injected embryos compared to control embryos was assessed in Fisher's exact test (see Materials and methods). No statistically significant differences were found between GFP-injected and Bcl-2-injected embryos at stage 19. At stage 23, differences between GFP-injected and Bcl-2-injected embryos were statistically significant in the most anterior (0–25%) and middle–posterior (51–75%) portions of the notochord, with grades 2 ($p=0.048$) and 1 ($p=0.048$) disruptions in Bcl-2-injected embryos, respectively. At stage 30, a significant difference between control and Bcl-2-injected embryos was only found in the anterior–middle region (26–50%) with grade 2 disruption ($p=0.015$) in the Bcl-2-injected embryos. By stage 35, significant differences between control and Bcl-2-injected embryos were found in the anterior (0–25%; $p=0.002$), anterior–middle (26–50%; $p=0.009$) and middle–posterior (51–75%; $p=0.009$) regions of the notochord with grade 2, 3 and 3 disruptions, respectively.

To further assess the loss of integrity of the notochord in Bcl-2-injected embryos with developmental stage, histological sections were examined at a higher magnification (Fig. 9). This revealed that at stage 23 the cells are similarly arranged in control and Bcl-2-injected embryos, although there is some disruption of notochord structure (compare Figs. 9A, A′, A″ to B, B′, B″, C, C′, C″). At stage 30, however, the structure of the notochord is severely compromised. While in control embryos the notochord has smooth edges and vacuolated cells, in Bcl-2-injected embryos it is kinked, its edges are broken and vacuoles are absent or irregularly shaped (compare Figs. 9D, D′, D″ to E, E′, E″, F, F′, F″). The disruption of notochord structure in Bcl-2-injected embryos is further exaggerated at stage 35, with no vacuolated cells (compare Figs. 9G, G′, G″ to H, H′, H″, I, I′, I″) and little or no discernable structure in bright field images (compare Figs. 9G, to H and I). The pattern of Tor70 immunostaining in later staged notochords suggested that the

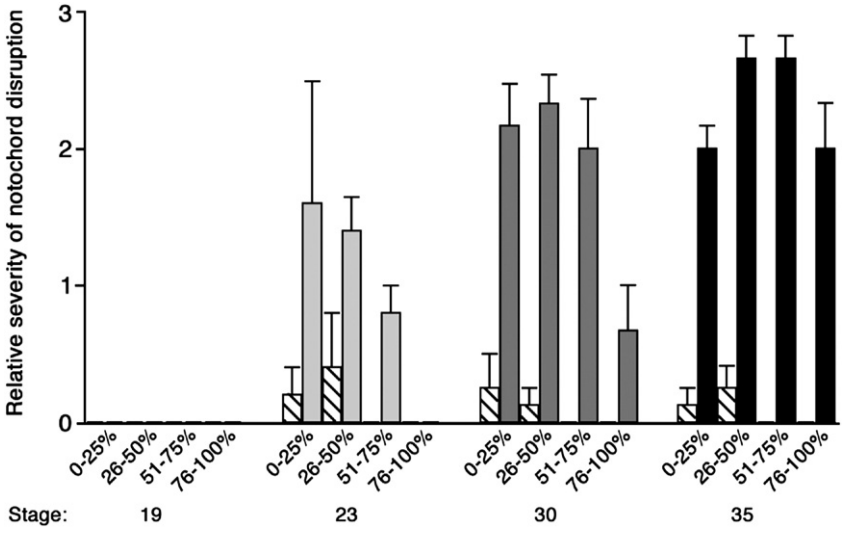

Fig. 8. Notochord structure is disrupted in an anterior to posterior progression with developmental stage when apoptosis is inhibited. Embryos were injected into the prospective notochord region with GFP mRNA (hatched bars) or Bcl-2 mRNA (solid bars) at the 4-cell stage. At stages 19, 23 (▫), 30 (▪) and 35 (■), the embryos were fixed, processed for immunohistochemistry using Tor70 and GFP antibodies, TUNEL stained and then embedded and sagittally sectioned. Notochord disruption was assessed in 4 different sectors that encompassed the percent of the notochord length from the anterior, 0–25%, 26–50%, 51–75% and 76–100%. The following values were used to score the severity of the phenotype, grade 0 for normal, grade 1 for a mild phenotype including a rippled notochord with contiguous borders, grade 2 for highly kinked notochord but with contiguous borders, and grade 3 for severe phenotypes including breakages in the notochord borders and a loss of structure. Note that, at stage 23, the notochord is disrupted only in the most anterior regions but at later stages, this disruption extends posteriorly such that by stage 35 the entire notochord is affected. Error bars indicate 95% confidence intervals. A minimum of 4 embryos in 3 independent experiments were used for this analysis.

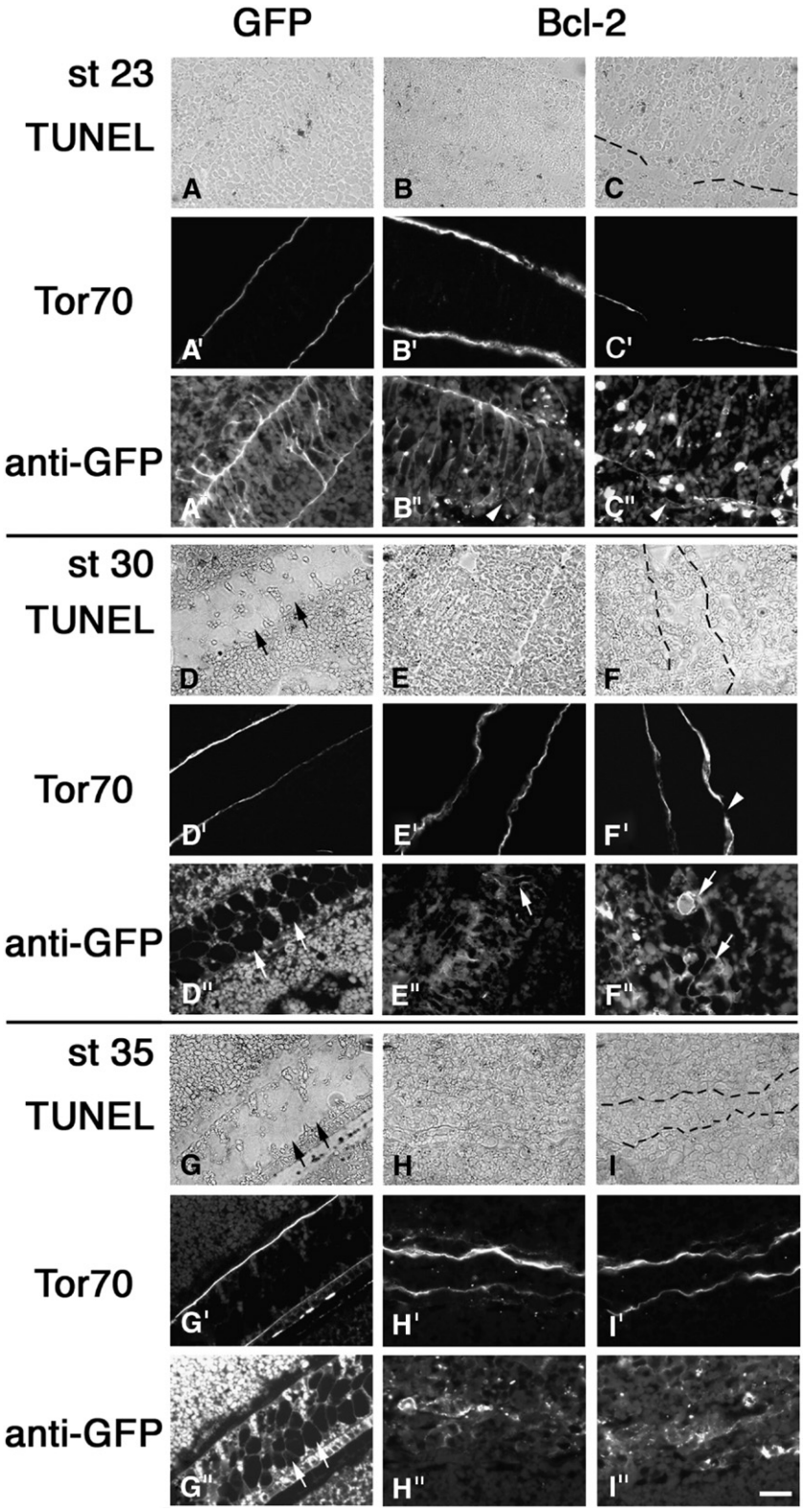

Fig. 9. Inhibition of apoptosis severely disrupts notochord structure. Embryos were injected into the prospective notochord region with (A, D, G) GFP mRNA or (B, C, E, F, H, I) Bcl-2 mRNA at the 4-cell stage. Two examples of Bcl-2-injected embryos are shown. At stages 23 (A–C), 30 (D–F) and 35 (G–I) the embryos were fixed, processed for immunohistochemistry using (A′–I′) Tor70 and (A″–I″) anti-GFP antibodies, (A–I) TUNEL stained and then embedded and sagittally sectioned. Note that inhibition of apoptosis caused the notochord to kink and develop with broken edges and with malformed or missing vacuoles. Arrows in panels D, D″, G and G″ point to vacuoles in wild type notochords. Compare to arrows in panels E″ and F″ that show misshapen vacuoles in Bcl-2-injected embryos. Arrowheads in panels B″, C″ and F′ indicate brakes in the notochord sheath. Dotted lines in panels C, F and I indicate the position of the notochord boundaries and correspond to frames panels C′, C″, F′, F″, I′ and I″. All frames taken at approximately the notochord anteroposterior midpoint. Anterior is to the left or down in all frames. Scale bar in panel I″ is 20 μm.

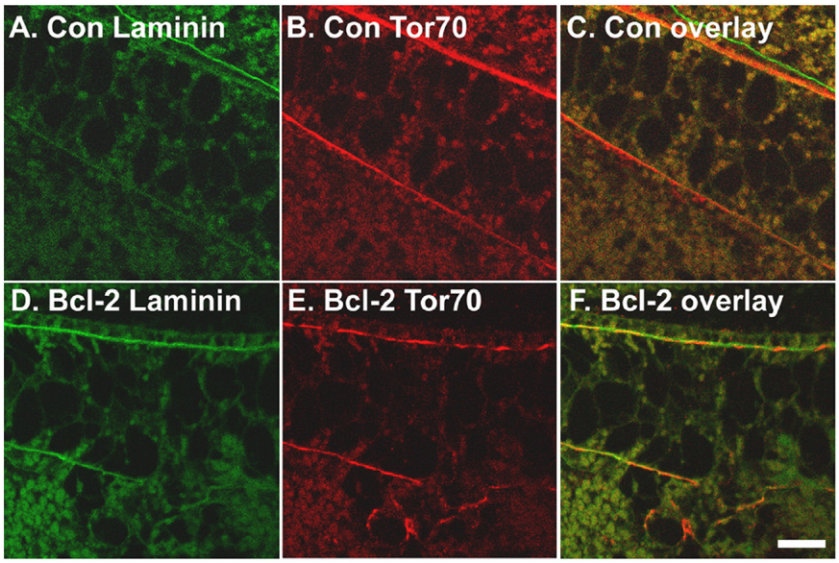

Fig. 10. The integrity of the sheath is compromised when apoptosis is inhibited in the notochord. Embryos were injected into the prospective notochord region with (A–C) GFP mRNA or (D–F) Bcl-2 mRNA at the 4-cell stage. At stage 35 the embryos were fixed, processed for immunohistochemistry using (A, D) anti-laminin and (B, E) Tor70 antibodies before being embedded and sagittally sectioned. Confocal microscopy (Axiovert LSM 200 M with 5 Pascal version 4 software; Zeiss) was used to analyze co-localization of the two markers (C, F) that outline the notochord, which overlapped 95–97%. Note that inhibition of apoptosis caused the notochord sheath to break. Anterior is to the left and dorsal is up in all frames. Scale bar in panel F is 40 μm.

notochord sheath was compromised when cell death was inhibited (for example, see Figs. 9F′, I′) and that although vacuoles appear to form initially, they are later lost (compare Figs. 9E″, F″ with H″, I″).

Laminin is an integral component of the peri-notochordal basement membrane that contributes to the sheath (Fey and Hausen, 1990; Parsons et al., 2002). In zebrafish mutants that lack either laminin β1 or γ1, the notochord sheath is disorganized and the number and size of the vacuoles are reduced (Parsons et al., 2002). Immunostaining of stage 35 Bcl-2-injected embryos revealed that laminin (Figs. 10A, D) co-localized with Tor70 (Figs. 10B, E, C, F) and that breaks are present in the notochord basement membrane (compare Figs. 10A with D), however, the amount of laminin appeared unchanged compared to controls.

This progression of notochord disruption with developmental stage and anterior–posterior position along the dorsal axis coincides with vacuolization and follows the spread of apoptosis in this tissue. This is suggestive of a mechanism in which kinking of the notochord in Bcl-2-injected embryos results from vacuolization of cells that would have normally been removed through apoptosis.

The temporal expression of notochord markers is not changed when apoptosis is inhibited

To determine whether a delay in notochord differentiation accounts for the observed phenotypes in Bcl-2-injected embryos, early and late notochord markers were examined by in situ hybridization. Analysis of control and Bcl-2-injected embryos at stage 23 indicated that the early marker AXPC and late marker procollagen IIA are expressed in the notochord (Figs. 11A, B and E, F, respectively). In later embryos, stages 35 and 37, the expression patterns of both AXPC (Figs. 11C, D) and procollagen IIA (Figs. 11G, H) are also identical in control and Bcl-2-injected embryos and correspond to those previously described (Kim et al., 1998; Su et al., 1991). AXPC is not expressed in the notochord at stage 35 but is found in the pronephros (Figs. 11C, D) and heart (not shown), whereas procollagen IIA expression is maintained in the notochord, suggesting that the temporal development of the notochord is not altered when apoptosis is inhibited.

Ectopic cell survival in the notochord causes disruptions in adjacent tissues

To examine whether ectopic cell survival in the notochord affected surrounding tissues, the neural tube and somites were examined at stage 35 by wholemount immunohistochemistry. Extension of both the neural tube and somites appeared to correspond to that of the notochord (Figs. 12A, B, E, F, I, J, M, N). For example, a shortened notochord in Bcl-2-injected embryos resulted in equivalently shorter anteroposterior axis, neural tube and somite file (compare Figs. 12E, M to F, N). In addition, disruption of notochord morphogenesis (Figs. 12G, O) resulted in somite and neural tube defects (Figs. 12H, P), compared to controls (Figs. 12C, D, K, L). It cannot be ruled out that neural tube defects may be the result of inhibiting apoptosis in this tissue (Hensey and Gautier, 1998). However, no apoptosis has been reported previously in the somites (Hensey and Gautier, 1998), which were highly disorganized in Bcl-2-injected embryos compared to controls (compare Figs. 13A and B). In embryos with the most severe notochord phenotype, in which the anterior is doubled back on itself towards the posterior (Fig. 12G), the somites do not follow this looping or extend beyond the anteroposterior length of the notochord (Fig. 12H).

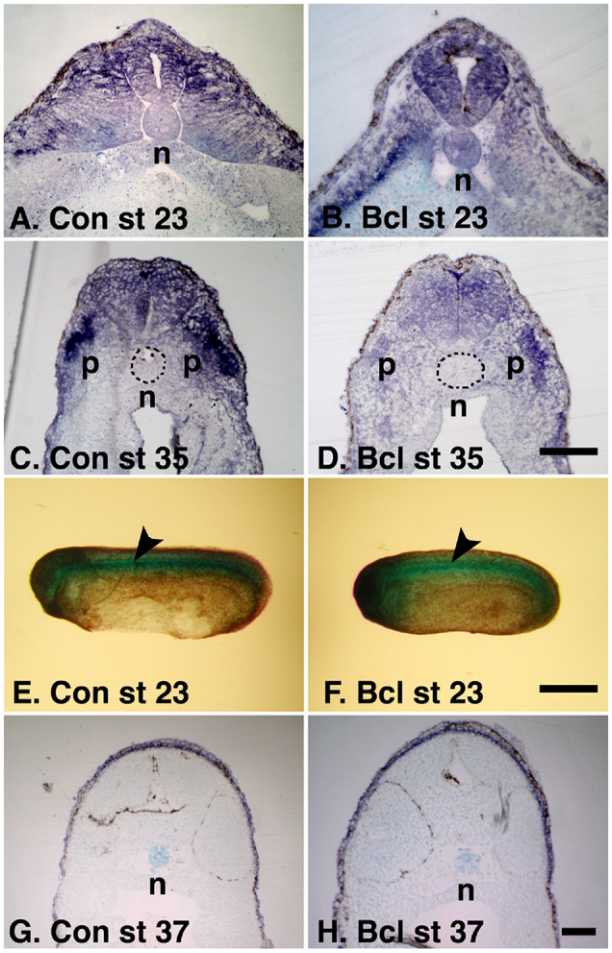

Fig. 11. The temporal expression of notochord markers is similar in control and Bcl-2-injected embryos. Embryos were injected into the prospective notochord region with (A, C, E, G) GFP mRNA or (B, D, F, H) Bcl-2 mRNA at the 4-cell stage. At stages 23 (A, B, E, F), 35 (C, D) and 37 (G, H) the embryos were fixed and processed for in situ hybridization using probes for AXPC (A–D) and procollagen IIA (E–H). The embryos were then photographed in wholemount (E, F) or embedded and transversely sectioned (A–D, G, H). Note that inhibition of apoptosis did not alter the pattern of expression of either marker. Notochord (n), pronephros (p). Dotted lines in panels C and D outline the notochord. Arrows in panels E and F point to the notochord. Anterior is to the left in panels E and F. Scale bar in panel D is 100 μm and applies to panels A–D, in panel F is 500 μm and applies to panels E and F and in panel H is 100 μm and applies to panels G and H.

Taken together, these data illustrate the essential role of apoptosis in regulating notochord development and suggest that the elimination of cells in this tissue may be necessary to compensate for the increase in cell volume during vacuolization and to coordinate the extension and proper differentiation of surrounding tissues.

Discussion

We have identified a new role for apoptosis, in the development of the notochord in *Xenopus*. We find that apoptotic cells in the notochord appear much earlier than previously reported. Cell death begins in the anterior notochord at stage 18 and the number of dying cells increases until at least stage 25. During this time, the distribution of apoptotic cells also changes, and the death spreads posteriorly with developmental stage. This period of development is critical for notochord formation in *Xenopus*. Previous studies have shown that between stage 21 and 25 the fiber density of the sheath increases as notochord cells undergo vacuolization, which allows the notochord to straighten and lengthen without being buckled by surrounding tissues (Adams et al., 1990). The apoptosis we observe in the notochord precedes but overlaps with vacuolization, which also spreads in an anterior to posterior fashion beginning at stage 23 and 24 (Adams et al., 1990).

Given these observations, one might predict that inhibition of apoptosis in the notochord would cause the tissue to elongate to a greater extent than normal. In open-faced Keller explants, this is the case. We found that inhibition of apoptosis by overexpression of Bcl-2 caused a significant increase in both the LWR of the explant and length of the notochord. In intact embryos, however, blocking cell death in the notochord caused a decrease in the anteroposterior length compared to controls, and the tissue was severely kinked. This apparent discrepancy between ex vivo and in vivo data might be due to differences in tissue environment. Explants are prevented from rounding up and healing by culturing them under a glass coverslip bridge. This allows mediolateral intercalation and convergent extension to occur in the plane of the tissue (Wilson et al., 1989). In these explants, the notochord is flanked by prospective somitic mesoderm and overlying suprablastoporal endoderm and lacks hindrance from surrounding tissues in the direction of extension, permitting the notochord to freely elongate during vacuolization. In the intact embryo, however, the notochord is also adjacent to the neural tube and archenteron roof, and embryo elongation is constrained in the direction of extension by the epidermis, which may provide sufficient resistance to notochord lengthening to cause kinking. Alternatively, differences in notochord length induced by Bcl-2 injection in ex vivo and in vivo conditions might result from changes in the notochord sheath, which is critical to notochord function, both in its role in embryo elongation (Keller, 2006; Koehl et al., 2000) and in its capacity as a signaling center (Stemple, 2005).

As a fiber wound, hydraulic system, the biomechanical properties of the notochord sheath affect the notochord's ability to change shape (Keller, 2006; Koehl et al., 2000) by resisting the tendency of the cells to swell during vacuolization (Adams et al., 1990). Using notochord models, it has been determined that the angle of extracellular matrix fibers in the sheath dictates whether on inflation (to mimic vacuolization) the notochord will narrow, lengthen and straighten or shorten and widen (Koehl et al., 2000). Fiber angles of greater than 54° with respect to the long axis caused narrowing and lengthening, whereas angles less than 54° resulted in shortening and widening (Koehl et al., 2000). In *Xenopus*, the angle of the extracellular matrix fibrils of the sheath is wound at approximately 54° (Adams et al., 1990). This suggests that even a small change in the angle of these fibers could alter whether the tissue lengthens and narrows or shortens and widens. Such a change might be brought about by a number of factors in Bcl-2-injected embryos such as an increase in cell number, dis-

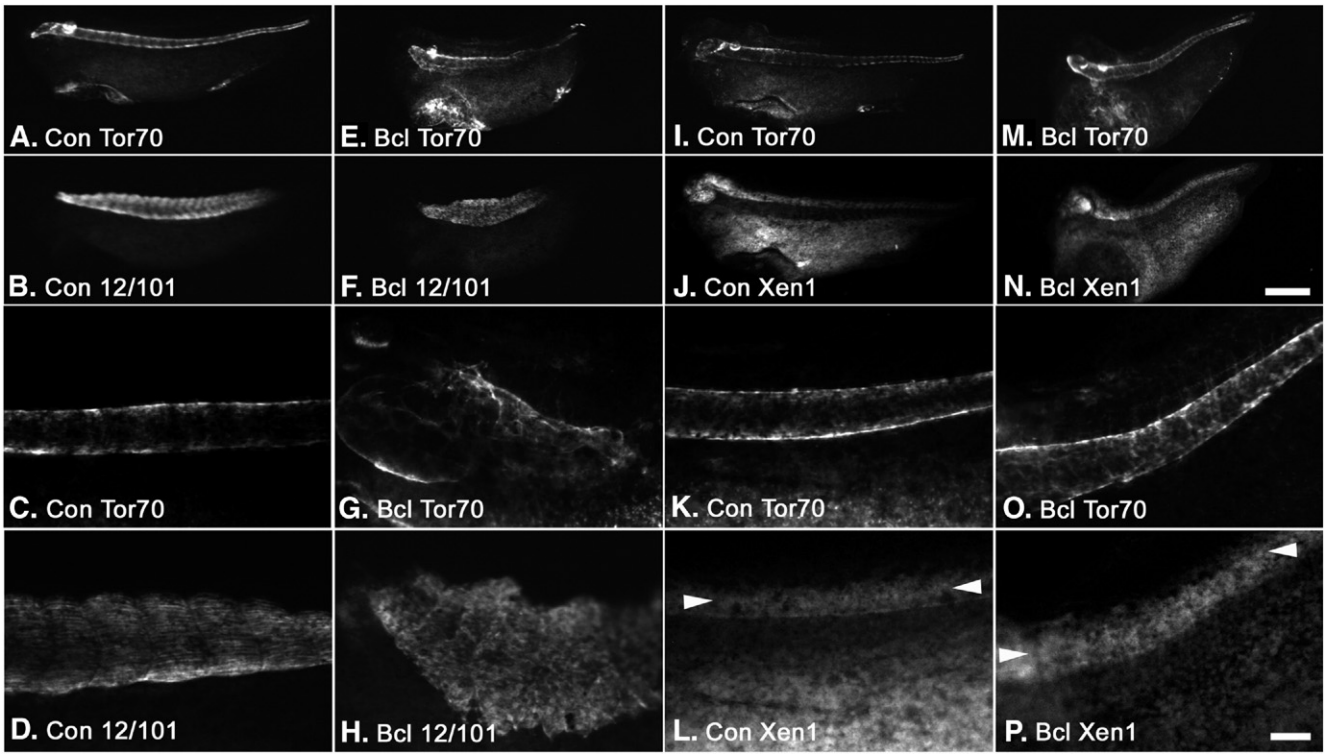

Fig. 12. Neural tube and somite extension mirrors that of the notochord. At stage 35, embryos that had been injected with GFP (A–D, I–L) or Bcl–2 (E–H, M–P) mRNA were subject to immunohistochemistry for notochord (A, C, E, G, I, K, M, O), skeletal muscle (B, D, F, H) or neural tube (J, L, N, P). Arrowheads in panels L and P indicate the neural tube. Anterior is to the left. Scale bar in panel N is 500 μm and applies to top 8 panels, and in panel P is 100 μm and applies to lower 8 panels.

organization of the cells, uneven inflation of vacuoles or increased internal pressure on vacuolization.

Notochord defects in Bcl-2-injected embryos also occur in an anterior to posterior pattern and increase in severity with developmental stage. These defects are correlated with the normal spread of vacuolization. The anterior notochord begins to kink at stage 23, the stage at which vacuolization is initiated. By stage 35, almost the entire notochord is vacuolated in control embryos, but in Bcl-2-injected embryos although vacuolization was initiated, previously formed vacuoles, and in some cases the entire notochord, appeared to collapse. The notochord was also kinked in these embryos and the disruptions spanned approximately the same area as the vacuoles in control embryos. These disruptions are accompanied by apparent breakages in the notochord sheath, and sheath disruptions may account for all observed defects when Bcl-2 is overexpressed in the notochord. For example, removal of the sheath in vitro by collagenase causes the cells to swell excessively and the developed notochord is severely kinked (Adams et al., 1990). In Bcl-2-injected embryos, breakages in the sheath might disrupt the normal balance of external fiber winding and internal osmotic pressure and cause the notochord to shorten and kink.

Zebrafish embryos mutant for genes encoding integral components of the notochord basement membrane such as

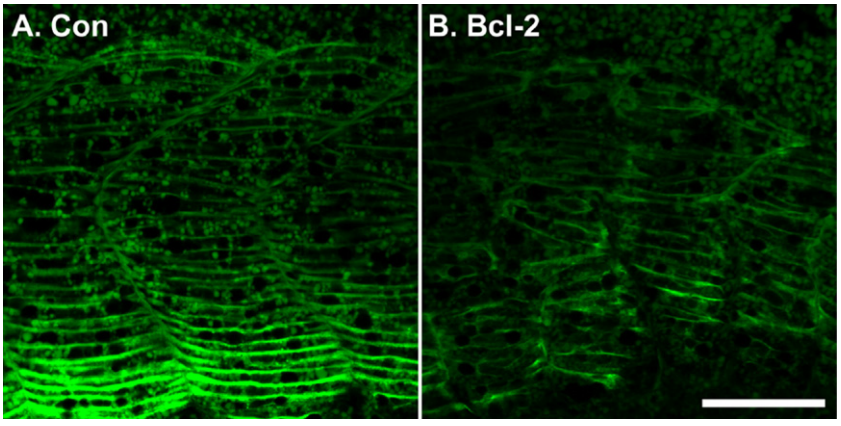

Fig. 13. Somites are disorganized when notochord apoptosis is inhibited. At stage 35, embryos that had been injected with GFP (A) or Bcl-2 (B) mRNA were subject to immunohistochemistry for skeletal muscle. Note severe disruption of somite structure in panel B. Anterior is to the left. Scale bar is 100 μm.

laminin have a shortened body axis and the notochord is kinked with only a few small vacuoles (Parsons et al., 2002). The notochord in these mutants also fails to differentiate and contains large numbers of apoptotic cells (Parsons et al., 2002). Bcl-2-injected embryos differ from these zebrafish mutants in that laminin appears to be present at similar levels to that in control embryos and notochord markers are expressed appropriately. The breakages in the sheath, however, may account for the loss of vacuoles and kinking of the notochord.

Notochord disruptions are also seen in *Xenopus* and zebrafish embryos when lysyl oxidase is inhibited (Anderson et al., 2007; Geach and Dale, 2005). In zebrafish embryos, β-aminopropionitrite, an inhibitor of copper-dependent lysyl oxidases, causes the notochord to undulate (Anderson et al., 2007). A similar phenotype is also seen in embryos with a copper deficiency (Mendelsohn et al., 2006). These undulations appear during the period of vacuolization and elongation, and the notochord develops with disrupted collagen fibrils (Anderson et al., 2007). Interestingly, lysyl oxidase inhibits NFκB (Jeay et al., 2003), which induces genes that prevent programmed cell death (Escarcega et al., 2007). Thus it is of interest to determine whether β-aminopropionitrite treatment increases cell survival in the notochord of these embryos.

While it is clear that apoptosis is required for normal notochord development, the precise role is not known. It is possible that it is used to remove damaged cells, perhaps injured by the 2- to 3-fold increase in internal pressure during vacuolization (Adams et al., 1990). For example, when dead cells are not removed by phagocytes in zebrafish embryos, the notochord deforms due to impeded cell migration and cell to cell communication (Hong et al., 2004). Alternatively, the apoptosis may regulate cell number during elongation and vacuolization. A similar mechanism of overproducing cells that are later eliminated by apoptosis is used in a number of developmental processes, for example, in the oligodendrocyte and neuron lineages in the vertebrate nervous system (Jacobson et al., 1997). Why apoptosis is used to regulate size as opposed to production of a precise number of cells is not understood. However, apoptosis may simply provide the more flexible mechanism in such a highly dynamic system, with the notochord approximately doubling in length between stages 23 and 28 (Adams et al., 1990), a period of about 8 h at room temperature (Nieuwkoop and Faber, 1967), in coordination with other tissues such as the epidermis.

The notochord disruptions in Bcl-2-injected embryos are accompanied by defects in the neural tube and somites, with both tissues shorter than those in control embryos and corresponding to the length of the notochord. This is not surprising as it is well established that these tissues depend upon the notochord for their extension (Elul and Keller, 2000; Ezin et al., 2003; Horstadius, 1944; Jacobson, 1981; Kitchen, 1938; Kitchen, 1949; Nieuwkoop, 1947; Reverberi et al., 1960). However, signals from the notochord are also essential for the formation and patterning of the neural tube and somites (Fleming et al., 2001; Wilson and Maden, 2005). The somites in Bcl-2-injected embryos are disorganized. It is unclear, however, whether this is due to a disruption of a biomechanical process or cell signaling, either of which might be perturbed when the sheath is broken. In the zebrafish laminin mutants, it is believed that laminin is not directly involved in the control of the notochord differentiation, but its loss leads to alterations in a basement membrane-associated signal (Parsons et al., 2002). In the absence of laminin, other important basement membrane components that are known mediators of growth factor activity in the notochord, such as keratan sulfate proteoglycan and aggrecan (Costell et al., 1999; Perrimon and Bernfield, 2000), are not properly organized. Both proteoglycans are normally localized to the peri-notochordal sheath (Domowicz et al., 1995; Smith and Watt, 1985), and it has been proposed that in the absence of peri-notochordal basement membrane, associated growth factor signaling is disrupted. In Bcl-2-injected embryos, the level of laminin does not appear to decrease, but the organization of the sheath is disrupted, and thus signals from the notochord may not be correctly delivered. Further studies are required to fully understand how notochord apoptosis affects its role as a signaling center. However, it appears that apoptosis is an essential component of normal notochord development that is necessary for it to function as a primitive skeleton.

Acknowledgments

We would like to thank the following people for their generous gifts of reagents and help. Richard Harland for Tor70, Kenn Albrecht for the laminin antibody and Eddie De Robertis for GAP43-GFP, AXPC and procollagen IIA. We would also like to thank Paul Toselli for help with histology, Vickery Trinkaus-Randall and Kathrin Kirsch for the use of their microscopes, Emilios Tahinci for help with dissection of the Keller explants and for scoring them double blind and Chao-Yu Guo and Henry Fourcade for help with statistics. We would also like to thank Erin Smith for careful reading of the manuscript. This work was supported by grants from the National Institutes of Health (RO1 CA 875375 to KS and AG00115 to MVS and MM).

Appendix A. Supplementary data

Supplementary data associated with this article can be found, in the online version, at doi:10.1016/j.ydbio.2007.08.047.

References

Adams, D.S., Keller, R., Koehl, M.A.R., 1990. The mechanics of notochord elongation, straightening and stiffening in the embryo of *Xenopus laevis*. Development 110, 115–130.

Anderson, C., Bartlett, S.J., Gansner, J.M., Wilson, D., He, L., Gitlin, J.D., Kelsh, R.N., Dowden, J., 2007. Chemical genetics suggests a critical role for lysyl oxidase in zebrafish notochord morphogenesis. Mol. Biosyst. 3, 51–59.

Aszodi, A., Chan, D., Hunziker, E., Bateman, J.F., Fassler, R., 1998. Collagen II is essential for the removal of the notochord and the formation of the intervertebral discs. J. Cell Biol. 143, 1399–1412.

Ataliotis, P., Symes, K., Chou, M.M., Ho, L., Mercola, M., 1995. PDGF signalling is required for gastrulation of *Xenopus laevis*. Development 121, 3099–3110.

Bolce, M., Hemmati-Brivanlou, A., Kushner, P., Harland, R., 1992. Ventral ectoderm of *Xenopus* forms neural tissue, including hindbrain, in response to activin. Development 115, 681–688.

Bruns, R.D., Gross, J., 1970. Studies on the tadpole tail: 1. Structure and organization of the notochord and its covering layers in *Rana catesbiana*. Am. J. Anat. 128, 193–224.

Christ, B., Huang, R., Wilting, J., 2000. The development of the avian vertebral column. Anat. Embryol. 202, 179–194.

Christ, B., Huang, R., Scaal, M., 2004. Formation and differentiation of the avian sclerotome. Anat. Embryol. (Berl) 208, 333–350.

Cleaver, O., Krieg, P.A., 2000. Notochord patterning of the endoderm. Dev. Biol. 234, 1–12.

Cole, L.K., Ross, L.S., 2001. Apoptosis in the developing zebrafish embryo. Dev. Biol. 240, 123–142.

Copp, A.J., Brook, F.A., Roberts, H.J., 1988a. A cell-type specific abnormality of cell proliferation in mutant (curly tail) mouse embryos developing spinal neural tube defects. Development 104, 285–295.

Copp, A.J., Corolla, J.A., Brook, F.A., 1988b. Prevention of spinal neural tube defects in the mouse embryo by growth retardation during neurulation. Development 104, 297–303.

Costell, M., Gustafsson, E., Aszodi, A., Morgelin, M., Bloch, W., Hunziker, E., Addicks, K., Timpl, R., Fassler, R., 1999. Perlecan maintains the integrity of cartilage and some basement membranes. J. Cell Biol. 147, 1109–1122.

Cotten, A., Sakka, M., Drizenko, A., Clarisse, J., Francke, J.P., 1994. Antenatal differentiation of the human intervertebral disc. Surg. Radiol. Anat. 16, 53–56.

Coucouvanis, E., Martin, G.R., 1995. Signals for death and survival: a two-step mechanism for cavitation in the vertebrate embryo. Cell 83, 279–287.

Coutinho, P., Parsons, M.J., Thomas, K.A., Hirst, E.M., Saude, L., Campos, I., Williams, P.H., Stemple, D.L., 2004. Differential requirements for COPI transport during vertebrate early development. Dev. Cell 7, 547–558.

Cunliffe, V.T., Ingham, P.W., 1999. Switching on the notochord. Gen. Dev. 13, 1643–1646.

Danos, M.C., Yost, H.J., 1995. Linkage of cardiac left–right asymmetry and dorsal-anterior development in *Xenopus*. Development 121, 1467–1474.

Dawson, B., Trapp, R.G. (Eds.), 2004. Basic and Clinical Biostatistics. Lange Medical Books/McGraw-Hill, New York.

Domowicz, M., Li, H., Hennig, A., Henry, J., Vertel, B.M., Schwartz, N.B., 1995. The biochemically and immunologically distinct CSPG of notochord is a product of the aggrecan gene. Dev. Biol. 171, 655–664.

Elul, T., Keller, R., 2000. Monopolar protrusive activity: a new morphogenic cell behavior in the neural plate dependent on vertical interactions with the mesoderm in *Xenopus*. Dev. Biol. 224, 3–19.

Escarcega, R.O., Fuentes-Alexandro, S., Garcia-Carrasco, M., Gatica, A., Zamora, A., 2007. The transcription factor nuclear factor-kappa B and cancer. Clin. Oncol. (R. Coll. Radiol.) 19, 154–161.

Ezin, A.M., Skoglund, P., Keller, R., 2003. The midline (notochord and notoplate) patterns the cell motility underlying convergence and extension of the *Xenopus* neural plate. Dev. Biol. 256, 100–114.

Fey, J., Hausen, P., 1990. Appearance and distribution of laminin during development of *Xenopus laevis*. Differentiation 42, 144–152.

Fleming, A., Keynes, R.J., Tannahill, D., 2001. The role of the notochord in vertebral column formation. J. Anat. 199, 177–180.

Fouquet, B., Weinstein, B.M., Serluca, F.C., Fishman, M.C., 1997. Vessel patterning in the embryo of the zebrafish: guidance by notochord. Dev. Biol. 183, 37–48.

Geach, T.J., Dale, L., 2005. Members of the lysyl oxidase family are expressed during the development of the frog *Xenopus laevis*. Differentiation 73, 414–424.

Glucksmann, A., 1951. Cell deaths in normal vertebrate ontogeny. Biol. Rev. 26, 59–86.

Goldstein, A.M., Fishman, M.C., 1998. Notochord regulates cardiac lineage in zebrafish embryos. Dev. Biol. 201, 247–252.

Goto, S., Uhthoff, H.K., 1986. Notochord action on spinal development. A histologic and morphometric investigation. Acta Orthop. Scand. 57, 85–90.

Hensey, C., Gautier, J., 1998. Programmed cell death during *Xenopus* development: a spatio-temporal analysis. Dev. Biol. 203, 36–48.

Hirata, M., Hall, B.K., 2000. Temporospatial patterns of apoptosis in chick embryos during morphogenetic period of development. Int. J. Dev. Biol. 44, 757–768.

Hong, J.R., Lin, G.H., Lin, C.J., Wang, W.P., Lee, C.C., Lin, T.L., Wu, J.L., 2004. Phosphatidylserine receptor is required for the engulfment of dead apoptotic cells and for normal embryonic development in zebrafish. Development 131, 5417–5427.

Horstadius, S., 1944. Uber die Folge von Chordaextirpation an spaten Gastrulae und Neurulae von Ambystoma punctatum. Acta Zool. Stolkh. 25, 75–88.

Jacobson, A.G., 1981. Morphogenesis of the neural plate and tube. In: Connelly, T.G., Brinkley, L., Carlson, B. (Eds.), Morphogenesis and Pattern Formation. Raven Press, New York, pp. 223–263.

Jacobson, M.D., Weil, M., Raff, M.C., 1997. Programmed cell death in animal development. Cell 88, 347–354.

Jeay, S., Pianetti, S., Kagan, H.M., Sonenshein, G.E., 2003. Lysyl oxidase inhibits ras-mediated transformation by preventing activation of NF-kappa B. Mol. Cell. Biol. 23, 2251–2263.

Keller, R.E., 1984. The cellular basis of gastrulation in *Xenopus laevis*: active postinvolution convergence and extension by mediolateral interdigitation. Am. Zool. 24, 589–603.

Keller, R., 2006. Mechanisms of elongation in embryogenesis. Development 133, 2291–2302.

Keller, R., Cooper, M.S., Danilchik, M., Tibbetts, P., Wilson, P.A., 1989. Cell intercalation during notochord development in *Xenopus laevis*. J. Exp. Zool. 251, 134–154.

Keller, R., Davidson, L.A., Shook, D.R., 2003. How we are shaped: the biomechanics of gastrulation. Differentiation 71, 171–205.

Kim, S.H., Yamamoto, A., Bouwmeester, T., Agius, E., DeRobertis, E.M., 1998. The role of paraxial protocadherin in selective adhesion and cell movements of the mesoderm during *Xenopus* gastrulation. Development 125, 4681–4690.

Kim, K.W., Kim, Y.S., Ha, K.Y., Woo, Y.K., Park, J.B., Park, W.S., An, H.S., 2005. An autocrine or paracrine Fas-mediated counterattack: a potential mechanism for apoptosis of notochordal cells in intact rat nucleus pulposus. Spine 30, 1247–1251.

Kintner, C.R., Brockes, J.P., 1984. Monoclonal antibodies identify blastemal cells derived from dedifferentiating limb regeneration. Nature 308, 67–69.

Kitchen, I.C., 1938. The effects of extirpation of the notochord undertaken at the medullary plate stage in *Ambystoma mexicanum*. Anat. Rec. 72, 34a.

Kitchen, I.C., 1949. The effects of notochordectomy in *Ambystoma mexicanum*. J. Exp. Zool. 112, 393–415.

Koehl, M.A.R., Quillin, K.J., Pell, C.A., 2000. Mechanical design of fiber-wound hydraulic skeletons: the stiffening and straightening of embryonic notochords. Am. Zool. 40, 28–41.

Kushner, P.D., 1984. A library of monoclonal antibodies to Torpedo cholinergic synaptosomes. J. Neurochem. 43, 775–786.

Lohr, J.L., Danos, M.C., Yost, H.J., 1997. Left–right asymmetry of a nodal-related gene is regulated by dorsoanterior midline structures during *Xenopus* development. Development 124, 1465–1472.

Mendelsohn, B.A., Yin, C., Johnson, S.L., Wilm, T.P., Solnica-Krezel, L., Gitlin, J.D., 2006. Atp7a determines a hierarchy of copper metabolism essential for notochord development. Cell Metab. 4, 155–162.

Morgan, R., Nalliah, A., Morsi El-Kadi, A.S., 2004. FLASH, a component of the FAS–CASPASE8 apoptotic pathway, is directly regulated by Hoxb4 in the notochord. Dev. Biol. 265, 105–112.

Mori, C., Nakamura, N., Kimura, S., Irie, H., Takigawa, T., Shiota, K., 1995. Programmed cell death in the interdigital tissue of the fetal mouse limb is apoptosis with DNA fragmentation. Anat. Rec. 242, 103–110.

Moriyoshi, K., Richards, L.J., Akazawa, C., O'Leary, D.D., Nakanishi, S., 1996. Labeling neural cells using adenoviral gene transfer of membrane-targeted GFP. Neuron 16, 255–260.

Münsterberg, A.E., Lassar, A., 1995. Combinatorial signals from the neural tube, floor plate and notochord induce myogenic bHLH gene expression in the somite. Development 121, 651–660.

Nakajima, K., Takahashi, A., Yaoita, Y., 2000. Structure, expression, and function of the *Xenopus laevis* caspase family. J. Biol. Chem. 275, 10484–10491.

Nieuwkoop, P.D., 1947. Experimental investigations on the origin and determination of the germ cells, and on the development of the lateral plates and germ ridges in Urodeles. Archs. Neerl. Zool. 8, 1–205.

Nieuwkoop, P.D., Faber, J. (Eds.), 1967. Normal Table of *Xenopus laevis* (Daudin). North-Holland Publishing Company, Amsterdam.

Odenthal, J., Haffter, P., Vogelsang, E., Brand, M., van Eeden, F.J., Furutani-Seiki, M., Granato, M., Hammerschmidt, M., Heisenberg, C.P., Jiang, Y.J., Kane, D.A., Kelsh, R.N., Mullins, M.C., Warga, R.M., Allende, M.L., Weinberg, E.S., Nusslein-Volhard, C., 1996. Mutations affecting the formation of the notochord in the zebrafish, *Danio rerio*. Development 123, 103–115.

Parsons, M.J., Pollard, S.M., Saude, L., Feldman, B., Coutinho, P., Hirst, E.M., Stemple, D.L., 2002. Zebrafish mutants identify an essential role for laminins in notochord formation. Development 129, 3137–3146.

Patterson, P.H., 1992. Neuron–target interactions. In: Hall, Z. (Ed.), An Introduction to Molecular Neurobiology. Sinauer Associates, Sunderland, MA, pp. 428–459.

Peng, H.B., 1991. Solutions and protocols. In: Kay, B.K., Peng, H.B. (Eds.), *Xenopus laevis*: Practical Uses in Cell and Molecular Biology, vol. 36. Academic Press, San Diego, pp. 657–662.

Perrimon, N., Bernfield, M., 2000. Specificities of heparan sulphate proteoglycans in developmental processes. Nature 404, 725–728.

Pourquie, O., Coltey, M., Teillet, M.-A., Ordahl, C., Le Douarin, N.M., 1993. Control of dorsoventral patterning of somitic derivatives by notochord and floor plate. Proc. Natl. Acad. Sci. U. S. A. 90, 5242–5246.

Raff, M.C., Barres, B.A., Burne, J.F., Coles, H.S., Ishizaki, Y., Jacobson, M.D., 1993. Programmed cell death and the control of cell survival: lessons from the nervous system. Science 262, 695–700.

Reverberi, G., Ortolani, G., Farinella-Ferruzza, N., 1960. The causal formation of the brain in the ascidian larva. Acta Embryol. Morphol. Exp. 3, 296–336.

Rufai, A., Benjamin, M., Ralphs, J.R., 1995. The development of fibrocartilage in the rat intervertebral disc. Anat. Embryol. 192, 53–62.

Ruiz i Altaba, A., 1992. Planar and vertical signals in the induction and patterning of the *Xenopus* nervous system. Development 116, 67–80.

Sater, A.K., Steinhardt, R.A., Keller, R., 1993. Induction of neuronal differentiation by planar signals in *Xenopus* embryos. Dev. Dyn. 197, 268–280.

Saunders, J.W., Fallon, J.F., 1966. Cell death in morphogenesis. In: Locke, M. (Ed.), Major Problems of Developmental Biology. Academic Press, New York, pp. 289–314.

Smith, J.C., Watt, F.M., 1985. Biochemical specificity of *Xenopus* notochord. Differentiation 29, 109–115.

Smits, P., Lefebvre, V., 2003. Sox5 and Sox6 are required for notochord extracellular matrix sheath formation, notochord cell survival and development of the nucleus pulposus of intervertebral discs. Development 130, 1135–1148.

Stemple, D.L., 2005. Structure and function of the notochord: an essential organ for chordate development. Development 132, 2503–2512.

Stemple, D.L., Solnica-Krezel, L., Zwartkruis, F., Neuhauss, S.C., Schier, A.F., Malicki, J., Stainier, D.Y., Abdelilah, S., Rangini, Z., Mountcastle-Shah, E., Driever, W., 1996. Mutations affecting development of the notochord in zebrafish. Development 123, 117–128.

Su, M.-W., Suzuki, H.R., Bieker, J.J., Solursh, M., Ramirez, F., 1991. Expression of two nonallelic type II procollagen genes during *Xenopus laevis* embryogenesis is characterized by stage-specific production of alternatively spliced transcripts. J. Cell Biol. 115, 565–575.

Tahinci, E., Symes, K., 2003. Distinct functions of Rho and Rac are required for convergent extension during *Xenopus* gastrulation. Dev. Biol. 259, 318–335.

Theiler, K., 1988. Vertebral malformations. Adv. Anat. Embryol. Cell Biol. 112, 1–99.

Van Stry, M., McLaughlin, K.A., Ataliotis, P., Symes, K., 2004. The mitochondrial-apoptotic pathway is triggered in *Xenopus* mesoderm cells deprived of PDGF receptor signaling during gastrulation. Dev. Biol. 268, 232–242.

Waddington, C.H., Perry, M.M., 1962. The ultrastructure of the developing urodele notochord. Proc. R. Soc. Lond., B 156, 459–482.

Wallingford, J.B., Ewald, A.J., Harland, R.M., Fraser, S.E., 2001. Calcium signaling during convergent extension in *Xenopus*. Curr. Biol. 11, 652–661.

Wilson, L., Maden, M., 2005. The mechanisms of dorsoventral patterning in the vertebrate neural tube. Dev. Biol. 282, 1–13.

Wilson, P., Oster, G., Keller, R., 1989. Cell rearrangement and segmentation in *Xenopus*: direct observation of cultured explants. Development 105, 155–166.

Yamada, T., Placzek, M., Tanaka, H., Dodd, J., Jessell, T.M., 1991. Control of cell pattern in the developing nervous system: polarizing activity of the floor plate and notochord. Cell 64, 635–647.

Yamada, T., Pfaff, S.L., Edlund, T., Jessell, T.M., 1993. Control of cell pattern in the neural tube: motor neuron induction by diffusible factors from notochord and floor plate. Cell 73, 673–686.

Yeo, W., Gautier, J., 2003. A role for programmed cell death during early neurogenesis in *Xenopus*. Dev. Biol. 260, 31–45.

Youn, B.W., Malacinski, G.M., 1981. Axial structure development in ultraviolet-irradiated (notochord-defective) amphibian embryos. Dev. Biol. 83, 339–352.

Zuzarte-Luis, V., Hurle, J.M., 2005. Programmed cell death in the embryonic vertebrate limb. Semin. Cell Dev. Biol. 16, 261–269.